Effective Use of CH₄ Gas as a Reducing Agent in Suspension Reduction Process

Woo-Il PARK and Sung-Mo JUNG*

Graduate Institute of Ferrous Technology (GIFT), Pohang University of Science and Technology (POSTECH), Cheongam-ro 77, Pohang, 790-784 Korea.

The current study investigated the reduction and carburization in the suspension reduction of the fine Chinese Benxi magnetite ore with CH_4-containing gas. A very high fractional reduction was achieved by CH_4-containing gas at 1 300°C compared with that by H_2 or CO gas. The reduction rate of the ore by CH_4 was higher than that by H_2 above 1 150°C. The activation energies of the ore reduction by 11 vol%CH_4 and 20 vol%H_2 were calculated to be 113.6 and 76.9 kJ/mol, respectively. The reduction mechanism analysis showed that the formation of thin Fe layer reduced from wustite and the carbon dissolved into metallic shell by carburization had great influences on the further reduction progress. It is believed that the subsequent progress is related to the formation of less dense shell of metallic Fe with some cracks by the building up of gas pressure at Fe/wustite interface. Furthermore, the synergistic effect of H_2 addition to CH_4 gas on the reduction of the magnetite ore was also clarified.

KEY WORDS: CH_4 gas; suspension reduction; carbon deposition; fractional reduction; reduction mechanism; synergistic effect.

1. Introduction

Although the blast furnace (BF) process currently produces more than 90% of the world's iron, it is expected to decrease by 15–20% between 1998 and 2015.[1] The decrease is mainly ascribed to environmental regulations and to the depletion of natural resources such as high grade iron ores and coking coals. Thus, it has been undertaken to develop alternative ironmaking processes using low grade iron ores and non-coking coals.

One of the ironmaking processes is the suspension reduction technology, which can extensively utilize fine iron ores, which results in the decrease of CO_2 generation in the ironmaking process. This technology is defined as the direct gaseous reduction of fine ore concentrates which are transported by reducing gases. The terminology, suspension has been used to represent the processes such as the "flash", "cyclone" and "in-flight" reduction. The process would use gaseous reducing agent such as hydrogen, natural gas, a reducing gas generated by the combustion of coal or waste plastics, or a combination of them.

Sohn et al.[2] suggested the suspension reduction technology of the following advantages: 1) no need for cokemaking, pelletizing or sintering, 2) use of high temperature, 3) possibility to produce either solid or molten iron, 4) few refractory problems, 5) easy feeding of the raw materials, 6) possibility of direct steelmaking in a single unit. They reported that the reduction rate of the fine particles in the suspension technology was sufficiently fast by H_2-containing gas. Nomura et al.[3] studied the rapid reduction of fine iron ores transported by CH_4. They reported that the reduction rate of ores in CH_4 gas is larger than that in H_2 gas with increasing the temperature due to carbon deposition. Some results are also contradictory regarding the effect of carbon deposition on the reduction reactions. In contrast with the conclusions by Read et al.,[4] Ostrovski and Zhang[5] demonstrated that the carbon deposition has a detrimental effect on the reduction reactions. However, most of the previous studies could not clearly explain the role of CH_4.

In the current study, the reduction of fine iron ores by CH_4-containing gas was investigated to clarify the role of CH_4 more clearly. In addition, the effect of the carburization in reduced Fe on the reduction progress of ore was also studied, which was used to examine the feasibility of CH_4 as a direct reducing agent in the direct reduced iron (DRI) production.

2. Experimental

2.1. Materials Preparation

Chinese Benxi ore containing some quartz and sulfur was used as raw ore which is a very fine magnetite concentrate that should otherwise be sintered or pelletized in the ordinary ironmaking processes. Since the magnetite ore is less reducible than hematite ore, it is a suitable ore for examining the feasibility of suspension reduction technology. **Table 1** shows the chemical composition of Chinese Benxi Magnetite. The ore particles were screened by the sieves and then checked by particle size analyzer. The sample ores of four sizes were used: 25–45 μm (mean diameter, 40 μm), 45–63 μm

Table 1. Chemical composition of Chinese Benxi magnetite ore.

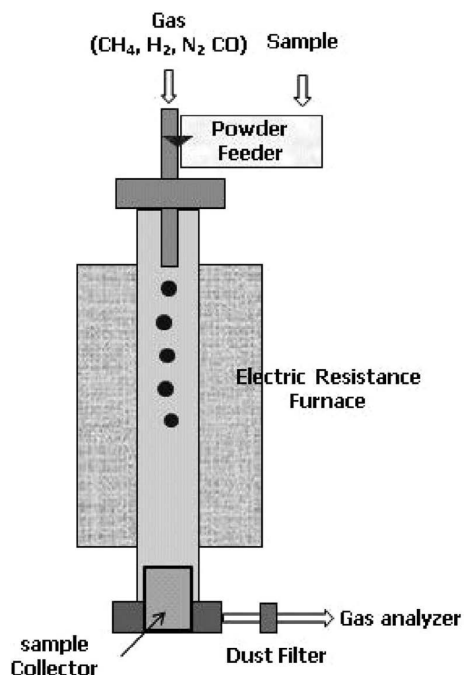|	Total Fe	FeO	Fe$_2$O$_3$	Metallic Fe	SiO$_2$	CaO	MgO	Al$_2$O$_3$	MnO	S	P
mass%	68.99	28.42	67.05	<0.1	4.9	0.12	0.3	0.089	0.052	0.21	0.012

Fig. 1. Schematic diagram of the experimental apparatus.

(mean diameter, 50 μm), 63–75 μm (mean diameter, 65 μm), 75–100 μm (mean diameter, 90 μm). The experiments were conducted using the particles of each size. However, the ore of 45–63 μm sample (mean diameter, 50 μm) was mainly used for the experiments of fixed particle size.

2.2. Experimental Apparatus and Procedure

Figure 1 shows the schematic diagram of an experimental apparatus. A drop-tube furnace is equipped with a commercial powder feeder (ROVO 2000) and a sample collector. The powder feeder is a screw type of a very sensitive rotational knife to precisely control the feed rate without clogging. The sample was fed downward at rates of 0.1 to 0.7 g/min and CO–N$_2$, H$_2$–N$_2$ or CH$_4$–H$_2$–N$_2$ gas mixtures transported the sample. The alumina reaction tube has the inner diameter of 25 to 60 mm and the length of 1 m. The isothermal zone within ±10°C is 0.13 m and the reduction temperature was changed from 1 150 to 1 460°C.

The concentrations of CH$_4$, CO and CO$_2$ in the off gas were measured by infrared gas analyzer (Fuji Instrument). In addition, the concentration of H$_2$ was measured by the thermal conductivity gas analyzer. The morphology and phases in the reduced products were identified with SEM, EPMA and XRD.

2.3. Estimation of Resident Time of In-flight Ore Particles

The resident time (τ) of ore particles determines the duration of suspension reduction. The resident time is calculated by varying the linear velocity of gas mixture (u_g), the length

Table 2. The resident time of the ore particle of 50 um as a function of tube diameter for 1.33×10^{-5} m^3/s of gas flow rate.

Tube diameter (mm)	25	40	50	60
Resident time (s)	0.38	0.58	0.65	0.70

of the reaction zone (L) and Stokes terminal velocity (u_s) under the assumption that the particles fall at a constant velocity in the reaction zone. Since the solid particles fall mainly near the center line, u_g is calculated by the maximum velocity, which is the twice the average velocity; volumetric flow rate divided by cross sectional area. The resident time (τ) is estimated by the following equations:[6]

$$u_p = u_g + u_s \quad \text{................................} \quad (1)$$

$$u_s = \frac{d_p^2 g \left(\rho_p - \rho_g \right)}{18 \mu} \quad \text{..........................} \quad (2)$$

$$\tau = \frac{L}{u_p} \quad \text{....................................} \quad (3)$$

where d_p = particle diameter (m), g = gravitational acceleration (9.81 m/s^2), ρ_p = particle density (kg/m^3), ρ_g = gas density (kg/m^3), u_p = particle velocity relative to tube wall (m/s), μ = gas viscosity (Pa·s). The viscosity of gas mixture (μ) is calculated by Wilke's equation.[7] One of the greatest advantages of suspension reduction is that the fine particle can be reduced within a few seconds or less than one second. It indicates that even a little resident time strongly affects the final reduction degree of the ores. Therefore, the resident time should be estimated and controlled appropriately in the reduction progress. Actually, the resident time is determined by several variables such as size and density of particles, flow rate of gases and tube diameter. Among them, the size of particles affects not only resident time but also surface area. In addition, high flow rate of gases may cause turbulent flow at the front of nozzle and low flow rate can generate a gas-limiting problem. Therefore, the resident time was controlled with changing the inner diameter of the reaction tube in the current study when the mean diameter of ore is 50 μm and the flow rate of gas is 1.33×10^{-5} m^3/s as shown in **Table 2**.

2.4. Evaluation of Fractional Reduction

After the reduction was finished, the reacted particles are transported downward and collected in the sample container. The fractional reduction of the reduced sample was estimated by Eq. (4) in terms of dimensionless number:

$$f = \frac{(O / Fe)_i - (O / Fe)_f}{(O / Fe)_i} \quad \text{......................} \quad (4)$$

where $(O/Fe)_i$ and $(O/Fe)_f$ are the initial and final mass ratios of oxygen to total iron in the sample, respectively, based on the results of chemical analyses.

3. Results

3.1. Effect of Gas Species on Fractional Reduction of Ore Particles

Haas *et al.*[8] already compared the reducibility of iron ores by H_2, CO and CH_4 in the temperature range of 800 to 1 100°C. Although H_2, CO and CH_4 rank in order of decreasing the reducing potential, it was reported that CH_4 has higher reducing potential than CO at 1 100°C. Steinfeld *et al.*[9] also compared the reducing potentials of the gases in the temperature range of 1 100 to 1 300°C. They also concluded that CH_4 reduced the ore much faster than H_2 or CO above 1 100°C. The current study found a similar tendency to the result by Steinfeld *et al.*[9] **Figure 2** shows the change in the fractional reduction of the magnetite ore with increasing the concentrations of the reducing gases at 1 300°C. Although CH_4 concentration is much smaller than that of H_2 or CO, it achieved a higher fractional reduction. CH_4 concentrations above 11 vol% achieved the fractional reduction of more than 0.7. However, H_2 gas could not reach the fractional reduction of 0.7 even with 50 vol%. Finally, CO gas
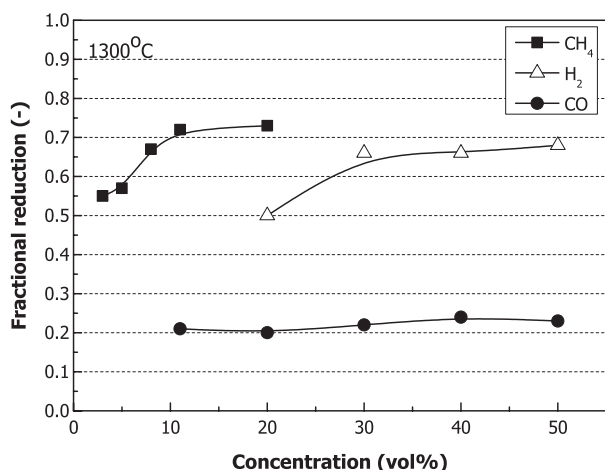
showed a much lower reducing potential than the other gases.

In addition, the gas mixture of 10 vol%CO and 20 vol%H_2 was examined to confirm whether the high reducing potential of CH_4 just resulted from the combination of CO and H_2 reduction or not. The fractional reduction of the ore by 10 vol%CO-20 vol%H_2 amounts to about 0.47 – 0.48, which are similar to those by 20 vol%H_2 gas, 0.46 – 0.53. This indicates that the reformed gas from CH_4 cannot provide such high reducing potential and that CH_4 itself must have an important role in the reduction mechanism, which will be dealt with in the discussion session.

3.2. Effect of Temperature on the Fractional Reduction of Ore Particles

Figure 3 shows the change in the fractional reduction of the ore by 11 vol%CH_4-N_2 from 1 150 to 1 300°C. The fractional reduction increased with increasing reduction temperature. In particular, there is large increase in the fractional reduction between 1 200 and 1 250°C while the change between 1 250 and 1 300°C is relatively small. This indicates that the temperature dependence of the reduction rate is comparatively high below 1 250°C, but the dependence is rapidly reduced above 1 250°C. It is believed that most of CH_4 gas was completely decomposed at between 1 200 and 1 300°C. Thus, the increase of temperature above 1 250°C has little effect on the cracking of CH_4. While the reformed H_2 gas is the dominant reductant at low temperatures, the active carbon might be a dominant reductant at high temperatures. Therefore, it is believed that the efficient temperature is around 1 250°C for the reduction of ore by CH_4 gas.

3.3. Effect of CH_4 Concentration on the Fractional Reduction of Ore Particles

Figure 4 shows that fractional reduction of the ore increased with increasing the content of CH_4 up to 8 vol%, but the fractional reduction little increased above 8 vol%. Steinfeld *et al.*[9] and Takeuchi *et al.*[6] previously reported the similar results in their experimental conditions. In addition, Ostrovski and Zhang[5] investigated the effect of CH_4 content on the reduction of various metal oxides. They commonly mentioned that the increase in CH_4 content up to 10 vol% enhanced the reduction rate of metal oxides. However,

Fig. 2. Change in the fractional reduction of the ores with increasing the concentration of CH_4, CO and H_2 in N_2 atmosphere at 1 300°C. (mean diameter of ore particles: 50 μm, resident time: 0.58 s).
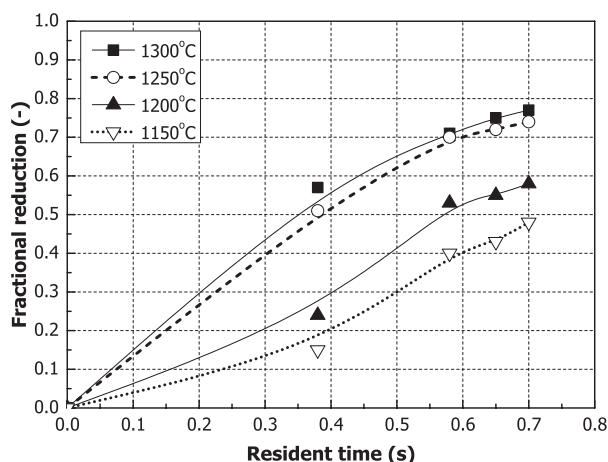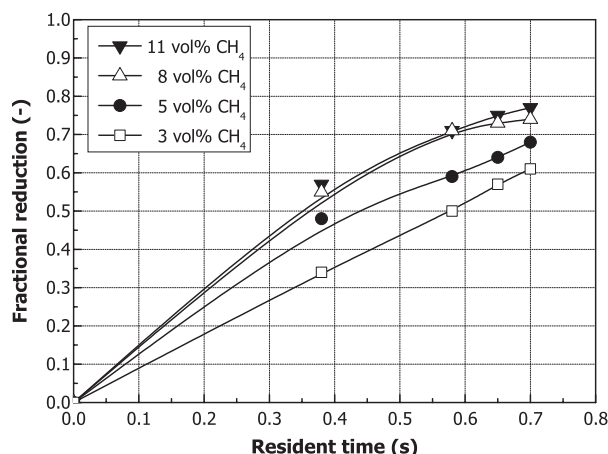

Fig. 3. Change in the fractional reduction of the ores with 11 vol%CH_4-N_2 in the temperature range of 1 150°C to 1 300°C.

Fig. 4. Effect of CH_4 concentration in N_2 atmosphere on the fractional reduction of the ore particles at 1 300°C.

excessive CH_4 content in the reducing gas resulted in the accumulation of solid carbon on the surface of ore particles, which ultimately retarded the reduction rate. Although the current study showed no retardation effect up to 11 vol% CH_4, high proportions of methane in the gas phase caused severe deposition of carbon on the reactor and experimental apparatus. It is believed that the formation of soot by CH_4 is the main drawback as a reducing gas at high temperatures.

3.4. Effect of H_2 and CO Addition on Fraction Reduction of Ore Particles

The effects of H_2 or CO addition to 11 vol%CH_4-N_2 gas mixture on the fractional reduction of the ore were examined at 1 300°C with increasing their concentrations from 0 to 50 vol%. As shown in the **Fig. 5**, while the increase in H_2 content gradually increased the fractional reduction, the addition of CO showed no noticeable effect. Ostrovski and Zhang[5] reported that CO gas had strong retarding effect on the reduction rate of metal oxides such as MnO, Cr_2O_3 and TiO_2, and that the retarding effect was ascribed to the reoxidation of carbides or CO adsorption onto the active sites of the oxide surface.[5] However, iron carbide was not formed
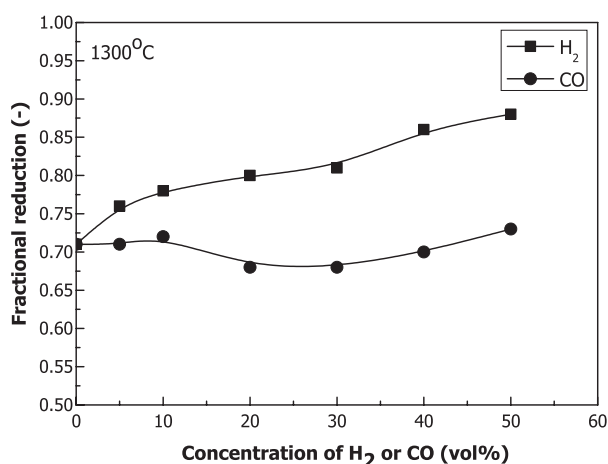
in the reduction taking place in less than 1 s in the current study considering that the formation of carbides took several hours by the previous researches.[5,10] The difference in the experimental conditions diminished the CO retardation effects in this study.

Because the admixing of CH_4 above 11 vol% or H_2 above 30 vol% did not effectively increase the fractional reduction of ore as shown in Fig. 2, it might be expected that very high fractional reduction can be achieved by mixing CH_4 and H_2. **Figure 6** shows the change in the fractional reduction of the magnetite ore by 20 vol%H_2, 11 vol%CH_4 and the mixture of 11 vol%CH_4 and 20 vol%H_2 in N_2 atmosphere at 1 300°C. The fractional reduction reached 0.9 when the mixture of CH_4 and H_2 was used for 0.7 s of resident time. This indicates that CH_4 and H_2 have a synergistic effect on the reduction rate, which will be discussed in detail later.

3.5. Effect of Particles Size on the Fractional Reduction of Ore Particles

The effect of particle size on the reduction was examined at 1 300°C. Although the feed rate of ore should be less than 0.13 g/min, the feeder could not operate constantly with larger particles unless the feed rate of ore was increased up to 0.17 g/min. **Table 3** shows the calculated resident time and fractional reduction evaluated by chemical analyses. As particle size increased from 40 to 80 μm, the resident time was reduced from 1.0 to 0.31 s. It is evident that the fractional reduction also decreased 0.84 to 0.64. Choi[11] similarly reported the effect of particle size on the suspension reduction of iron ore by H_2. That is, the equivalent fractional reduction were achieved at much lower temperatures with the smaller particles of ore in the similar range of resident time. However, the results obtained in the current study show that the fractional reduction by CH_4-containing gas was relatively less affected by particle size than that by H_2 suspension reduction. This indicates that the suspension reduction by CH_4 is much more effective than that by H_2.

3.6. Carburization of Reduced Metallic Shell

Although the resident time of in-flight ore particles in the current study was less than 1 s, CH_4 could effectively carburize the reduced metallic shell unlike H_2 or CO gas. **Figure 7** illustrates the carbon concentration in the reduced metallic shell with varying CH_4 content and resident time at 1 300°C. The carbon content was evaluated by EPMA quantification. Tacheuchi et al.[6] previously investigated the carbon concentration in the metallic shell reduced from wustite

Fig. 5. Effects of H_2 and CO addition to 11 vol%CH_4-N_2 gas mixture on the fractional reduction of ore at 1 300°C. (mean diameter of ore particles: 50 μm, resident time: 0.58 s).
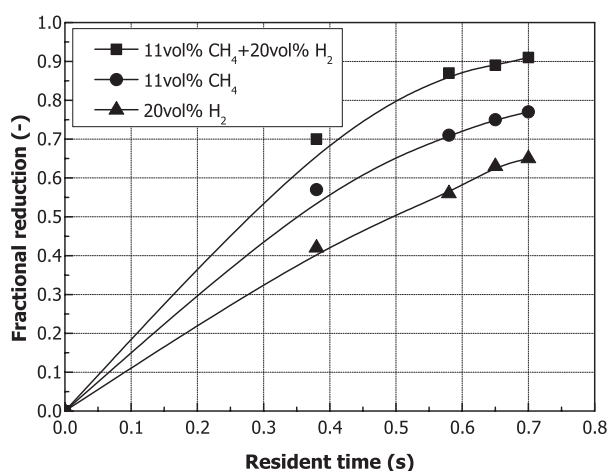

Fig. 6. Change in the fractional reduction of ore by 20 vol% H_2, 11 vol% CH_4 and 11 vol% CH_4+20 vol% H_2 balanced with N_2 atmosphere at 1 300°C.

Table 3. Effect of particles size on the calculated resident time and fractional reduction of the ore by 11 vol%CH_4-20 vol%H_2-N_2 at 1 300°C. (Gas flow rate: 1.33×10^{-5} m³/s, ore feed rate: 0.17 g/min, tube diameter: 60 mm).

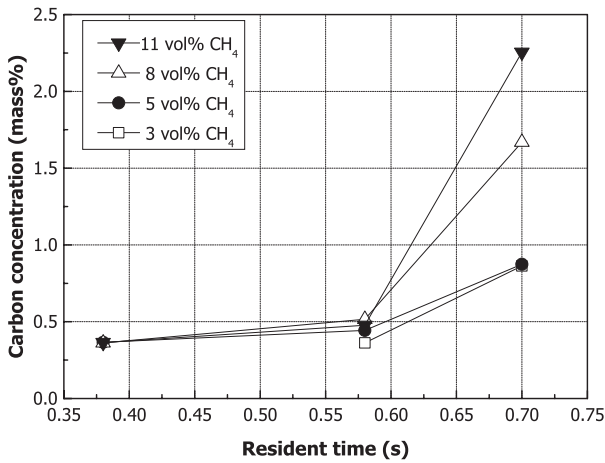| Particle size (μm)	mass%			Resident time (s)	Fractional reduction (−)
	Total Fe	Metallic Fe	FeO		
25–45 (40)	84.58	67.36	19.86	1.00	0.84
45–63 (50)	80.65	61.42	22.78	0.70	0.81
63–75 (65)	80.11	56.92	27.09	0.45	0.77
75–100 (80)	72.74	38.32	44.29	0.31	0.64

Fig. 7. Carbon concentration in reduced metallic shell with varying CH₄ content and resident time at 1 300°C.
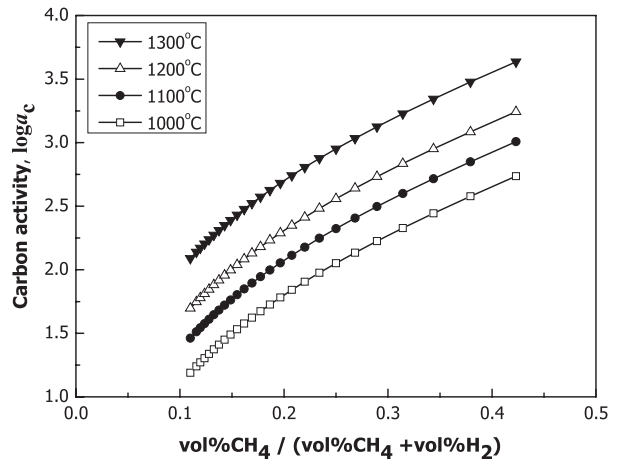

Fig. 8. Change in the calculated activity of carbon with varying H₂ content at 11 vol% CH₄ in CH₄–H₂–N₂ mixed gas in the temperature range of 1 000 to 1 300°C.

with changing CH₄ concentration. They obtained very high carbon concentrations of about 4 mass% when using 11 vol% CH₄ even though the resident time was less than 0.5 s. In the present study, however, the carbon concentration within 0.58 s of resident time were less than 0.5 mass% regardless of CH₄ content. When H₂ gas was used as a reducing gas, the carbon concentration in the metallic shell was about 0.4 mass%, indicating that the carburization did not strongly occur within 0.58 s. It is believed that the difference between the current results and those by Tacheuchi *et al.*[6] might be ascribed to the role of H₂. While the magnetite reduced to wüstite, H₂ dominantly reacted with oxygen in the ore to produce water vapor. The water vapor then reacted with carbon on the reaction surface of the metallic Fe by the following water-gas reaction. It is well known that this reaction is endothermic and sufficiently fast above 1 000°C.[12]

$$C(s) + H_2O(g) \rightarrow CO(g) + H_2(g) \quad \text{............ (5)}$$
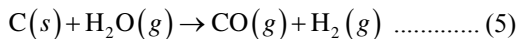
On the other hand, when the resident time was 0.7 s, the carbon concentration rapidly increased with increasing the CH₄ content. That is, the metallic shells formed by the reduction with 8 and 11 vol% CH₄ were located in the phase between the liquidus and solidus lines. Therefore, it can be fully expected that the metallic shell formed by the ore reduction with 3 and 5 vol% CH₄ might be a solid phase.

4. Discussion

4.1. High Activity of Carbon Produced by CH₄ Cracking

The decomposition steps of CH₄ on the active sites of the reaction surface were already illustrated in the carburization study by Grabke:[13]

$$CH_4(g) = \underline{C} + 2H_2(g) \quad \text{..................... (6)}$$
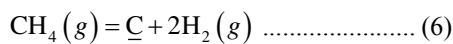
The carburization reaction (6) comprises the following seven reactions.

$$
\begin{array}{llll}
CH_4(g) & = & CH_{4(ad)} & \text{(I)} \\
CH_{4(ad)} & = & CH_{3(ad)} + H_{(ad)} & \text{(II)} \\
CH_{3(ad)} & = & CH_{2(ad)} + H_{(ad)} & \text{(III)} \\
CH_{2(ad)} & = & CH_{(ad)} + H_{(ad)} & \text{(IV)}
\end{array}
$$

$$
\begin{array}{llll}
CH_{(ad)} & = & C_{(ad)} + H_{(ad)} & \text{(V)} \\
H_{(ad)} & = & H_2 & \text{(VI)} \\
C_{(ad)} & = & \underline{C} & \text{(VII)}
\end{array}
$$

It has been already known that Step III is the rate-determining step, and then the rate of reaction can be represented by the following equation in the unit of mol·cm⁻²·s⁻¹:

$$v = k \cdot \frac{p_{CH_4}}{p_{H_2}^{1/2}} - k^* \cdot p_{H_2}^{3/2} \cdot \Gamma_c \quad \text{..................... (7)}$$

Steps (I) to (VI) among the above steps indicate the adsorption and decomposition of CH₄, and can be presented by the following Reaction (8):

$$CH_4 \rightarrow \cdots \rightarrow C_{(ad)} + 2H_2(g) \quad \text{.................. (8)}$$
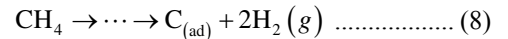
where C₍ad₎ represents the active carbon adsorbed on the reaction surface, which is totally different from solid carbon deposited. The activity of adsorbed carbon, aC can be calculated by Eq. (9):

$$a_C = K\left(p_{CH_4} / p_{H_2}^2\right) \quad \text{......................... (9)}$$

where *K* is the equilibrium constant of the graphite deposition reaction (10).

$$CH_4(g) = C_{(gr)} + 2H_2(g) \quad \text{.................. (10)}$$
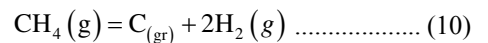
$$\Delta G^\circ = 91,040 - 110.7T \ (J/mol)^{14)} \quad \text{.............(11)}$$

Figure 8 shows the change in the calculated activity of carbon with varying H₂ content for 11 vol% CH₄ in CH₄–H₂–N₂ mixed gas. As expected from the thermodynamic data by Eq. (11), the carbon activity increases with increasing temperature and with decreasing H₂ content. In particular, the larger increase of carbon activity with increasing temperature from 1 200 to 1 300°C can explain the rapid improvement in the fractional reduction with increasing temperature from 1 200 to 1 250°C in Fig. 3. The high activity of carbon from CH₄-containing gas might be the great driving force for the fast reduction rate since the high reactivity of carbon provides favorable thermodynamic condition for reduction. However, if the carbon consumption by carburization or reduction is overwhelmed by the deposition of solid carbon on the surface, the carbon activity decreases to unity and rather blocks the access of the reducing gas to the ore, which

have no thermodynamic advantage compared with the conventional carbothermic reduction of ore. As a matter of fact, the reduction of carbon-coated iron ore was examined by Sugawara *et al.*[15] Although most of the experimental conditions in Sugawara *et al.*[15] were similar to those in the current study, they achieved a much lower fractional reduction of 0.38 for the resident time of 0.7 s. This might be ascribed to the limited access of H_2 gas to the reactive site on the surface of metallic Fe shell covered by the carbon particles of low reactivity.

4.2. Mechanism and Kinetics of the Suspension Reduction of Magnetite Ore

It is generally known that the reduction in wustite to iron is much slower than that in magnetite to wustite. The rate constant can be determined from the slowest step in the whole reduction process.[9] Therefore, it can be assumed that the following chemical reactions determine the rate of reduction in the current study:

$$FeO(s) + CO(g) = Fe(s) + CO_2(g) \quad .... (12)$$

$$FeO(s) + H_2(g) = Fe(s) + H_2O(g) \quad .... (13)$$

$$FeO(s) + \underline{C}_{in\,Fe} = Fe(s) + CO(g) \quad .... (14)$$
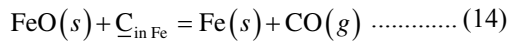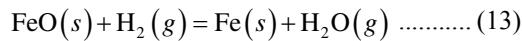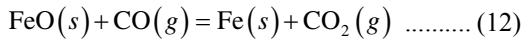
Since CO gas is not effective for reducing the ore concentrate in the current study, the rate analysis was focused on Reactions (13) and (14). In the case of fine concentrate ore, it was reported that the rate-controlling step is the chemical reaction at the iron/oxide interface according to the previous researches.[3,6,11] Therefore, it was attempted to apply the unreacted core model for the rate analysis using the rate equation for a spherical solid particle proposed by Szekely *et al.*[16] In case the reduction is controlled by chemical reaction in a topochemical reduction manner, the relationship between the fractional reduction and time is described by Eq. (15):

$$1 - (1-f)^{1/3} = \frac{k_1 t}{r_0 d_0} \quad .... (15)$$

where f is the fractional reduction, and r_0, d_0, k_1 and t are the mean radius of initial sample, molar concentration of removable oxygen in sample, apparent reaction rate constant and time, respectively. **Figure 9**(a) shows that relatively linear relationships between $1-(1-f)^{1/3}$ and resident time were found for the case of low CH_4 concentrations except for some data points measured at longer resident time for 8 and 11 vol% CH_4. All the data points correspond to the reduction stage where wustite is being reduced to Fe if taking into account of the fraction reduction of 0.25 where all the magnetite transforms to wustite. The results indicate that the initial reduction of wustite is carried out by H_2 gas in a topochemical reduction manner. However, since the dense Fe layer is impervious to the diffusion of H_2 once Fe layer becomes thicker on the surface of wustite, it is believed that the subsequent reduction of wustite would be carried out by the dissolved carbon in Fe layer. That is, according to Eq. (14), the remaining reduction of wustite would be performed just like the carbothermic reduction of wustite by dissolved carbon. Therefore, it was undertaken to apply the uniform internal reduction model,[17] and to plot the data for the frac-
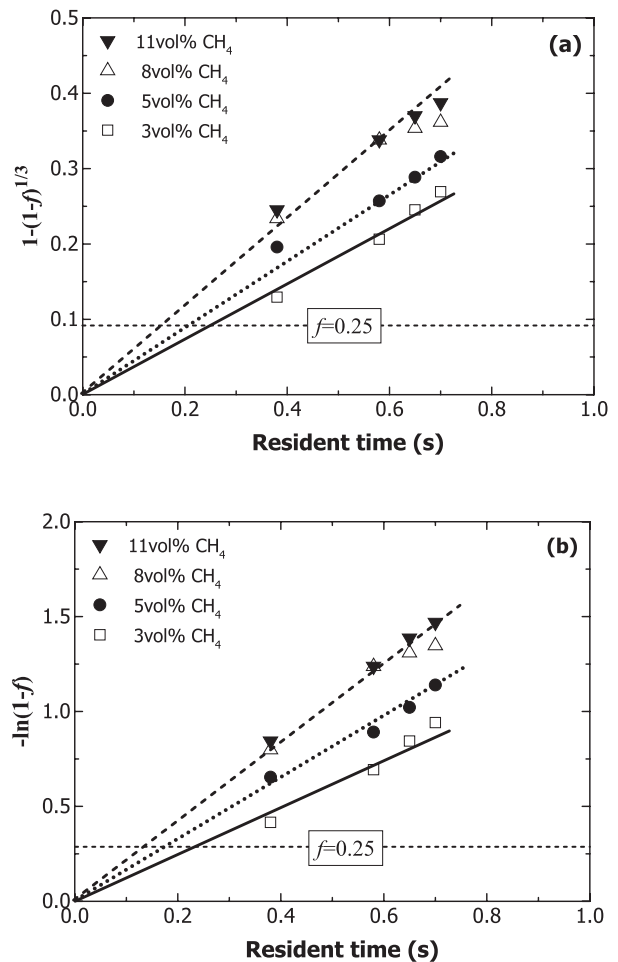

Fig. 9. Relationship between (a) $1-(1-f)^{1/3}$ and (b) $-\ln(1-f)$ and resident time in the reduction of magnetite ore with varying CH_4 concentration at 1 300°C.

tional reduction, f & rate constant, k_2 (1/s) as shown in Fig. 9(b), which showed better linear relationship with the resident time compared with that in Fig. 9(a):

$$-\ln(1-f) = k_2 t \quad .... (16)$$

The results in Fig. 9(b) implies that the reduction mechanism is changed over to the reduction of wustite by dissolved carbon from that by H_2 right after some thin Fe layer was formed on the surface of wustite. In addition, this strongly indicates that the reduction of wustite by dissolve carbon is limited by the gasification of dissolved carbon at Fe/wustite interface since the model was derived under the assumption that the overall reduction rate is controlled by carbon gasification. That is, Reaction (14) proceeds through the intermediate gases, CO and CO_2 in terms of Eqs. (17) and (18):[17]

$$FeO(s) + CO(g) = Fe(s) + CO_2(g) \quad .... (17)$$

$$\underline{C}_{in\,Fe} + CO_2(g) = 2CO(g) \quad .... (18)$$
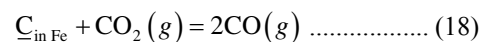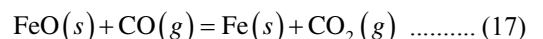
In general, it has been reported that CO consumption rate in the reduction of iron ore is larger than CO generation rate by non-catalytic oxidation of coke.[18] However, the reduction rate of wustite might be equal or smaller than the gasification rate by dissolved carbon with increasing temperature above 1 250°C. Furthermore, the reactivity of dissolved carbon

could have extremely increased since it originated from the active carbon adsorbed on the surface of metallic Fe.

The rate-controlling step can complementarily be estimated by the magnitude of the activation energy values.[19] The activation energy of the reaction can be determined by Arrhenius's Eq. (19):

$$k = k_0 \exp\left(-E_A / RT\right) \quad \text{.....................} \quad (19)$$

The apparent rate constants, k_1 (mol·m^{-2}·s^{-1}) and k_2 (1/s) were evaluated by analysis using the data of 20 vol%H$_2$ and 11 vol%CH$_4$, respectively, and then they were plotted against the reciprocal of absolute temperature as shown in **Fig. 10**. From the slope of the straight line in Fig. 10, the activation energies of the reductions by CH$_4$ and H$_2$ were calculated to be 113.6 and 76.9 kJ/mol, respectively. This indicates that the reduction by CH$_4$ is much more temperature dependent than that by H$_2$. Ghosh et al.[20] previously reported that H$_2$ reduction was the dominant reducing pathway of the CH$_4$ reduction in the temperature range of 800 to 1 025°C. The data in Fig. 10 clearly showed that the rate constants of CH$_4$ and H$_2$ crossed in between 1 200 and 1 250°C. This result is similar to that obtained at 1 100°C by the previous researches.[8,9] The activation energy value of 113.6 kJ/mol is slightly smaller than those by CO gas which ranges from 116 to 151 kJ/mol,[21–23] and is much smaller than 192.5 kJ/mol evaluated by Nomura et al.[3] and 214.3 kJ/mol reported by Takeuchi et al.[6] This might be ascribed to the assumption made in the current study that the difference in the activation energy resulted from the difference in the phase of the outer metallic shell. Takeuchi et al.[6] obtained a liquid metallic shell at 1 300°C and mentioned about the effect of CO/CO$_2$ bubble in the Fe layer. However, the phase in the present study was located below the liquidus line, and there was no obvious bubble layer at the interface. In addition, the activation energy of 113.6 kJ/mol was nearly close to 112.2 kJ/mol reported by Takeuchi et al.[6] for the solid metallic shell. This indirectly implies that the Fe layer is in the solid state in the progress of reduction, in particular, in the fractional reduction higher than 0.25. Therefore, it is believed that the reduction of wustite by dissolved carbon in the solid Fe layer could be limited by the reduction of wustite by CO, Eq. (17).
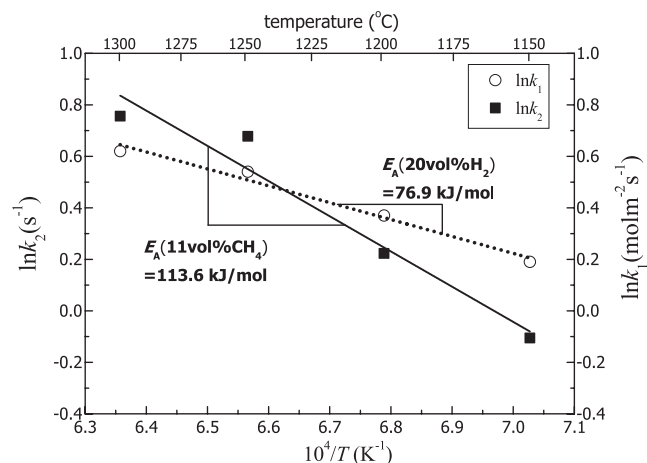
4.3. Suspension Reduction Progress of Magnetite Ore by CH$_4$

Nomura et al.[3] and Takeuchi et al.[6] previously proposed the mechanism of ironmaking by CH$_4$-containing gas. They suggested that the reduction of wustite progresses by diffused carbon and that the shell of metallic Fe grows up topochemically. However, the diffused carbon in the metallic shell alone cannot explain the low carbon concentrations in Fig. 7 and the effect of H$_2$ addition as well as the results by Sugawara et al.[15] for the reduction of carbon-coated iron ore. The mechanism should be modified in such a way that the morphology of the particle reduced by CH$_4$ is critically different from that reduced by H$_2$. Therefore, as shown in **Fig. 11**, the cross sections of the samples reduced by H$_2$ and CH$_4$ were observed with FE-SEM, respectively.

As shown in Fig. 11(a), relatively continuous, thin and dense Fe layer of about 5 μm in thickness was formed on the surface of wustite in the case of H$_2$ reduction, whose phenomena were previously reported.[19,24] Starting with a dense sphere of magnetite, an initial reduction by H$_2$ will produce a metallic Fe layer in contact with a layer of wustite beyond which there might be a layer of magnetite according to the so-called topochemical reduction pattern:[19]
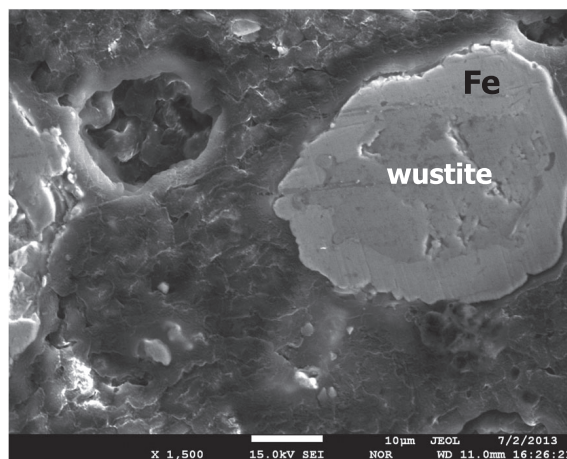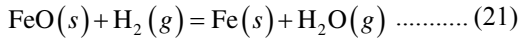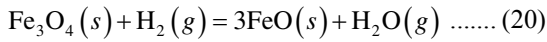

(a) A product particle reduced by H$_2$
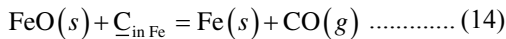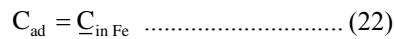(A planar Fe/FeO interface)
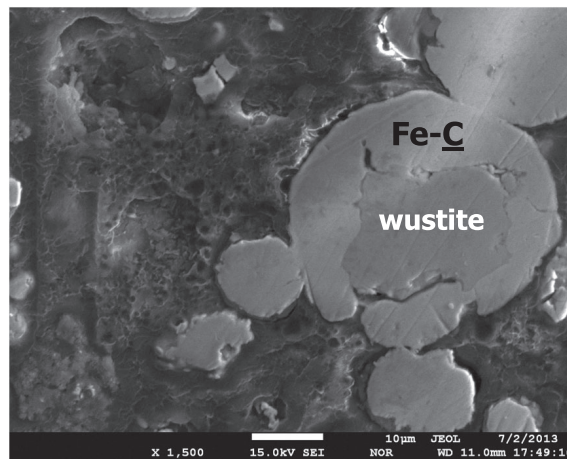
(b) A product particle reduced by CH$_4$
(A breakdown of the metal layer)

Fig. 11. SEM images of the cross sections of the samples reduced by (a) H$_2$ and (b) CH$_4$ at 1 300°C.

Fig. 10. Temperature dependence of the apparent reaction rate constant in the temperature range of 1 150 to 1 300°C.

$$Fe_3O_4(s) + H_2(g) = 3FeO(s) + H_2O(g) \quad \text{.......} (20)$$

$$FeO(s) + H_2(g) = Fe(s) + H_2O(g) \quad \text{..........} (21)$$

Right after the thin, dense and impervious layer of Fe was formed on the surface of wustite from magnetite ore, the reduction rate by H_2 slowed down as shown in Figs. 2 and 6. That is, the reduction of ore by H_2 would become stagnated in the reduction progress from wustite to metallic Fe. This is because even the thin layer of Fe formed can easily hinder the supply of H_2 gas to the reaction interface.

As shown in Fig. 11(b), the similar Fe layer was formed on the surface of wustite in the case of CH_4 reduction. However, compared with the Fe layer formed by H_2 reduction, a little thicker layer of Fe–C was in loose contact with the unreduced wustite according to the topochemical reduction pattern.[19] This is ascribed to the continuous dissolution of adsorbed carbon into the Fe layer formed by H_2 reduction, then the wustite is reduced by the dissolved carbon in Fe layer at Fe/wustite interface by Eqs. (22) and (14):

$$C_{ad} = \underline{C}_{\text{in Fe}} \quad \text{..............................} (22)$$

$$FeO(s) + \underline{C}_{\text{in Fe}} = Fe(s) + CO(g) \quad \text{.............} (14)$$

In addition, there exist some cracks and voids in Fe layer, which might result in making the Fe layer discontinuous, and the Fe layer is not in tight contact with unreduced wustite. This is due to the pressure building up of gases generated by the previous reaction.

Figure 12 illustrates the suggested reduction mechanism by CH_4: In Step (1), the magnetite is rapidly reduced to wustite by H_2 provided by CH_4 cracking. In Step (2), H_2 reduces wustite to metallic Fe to generate H_2O and the adsorbed carbon dissolves into Fe. First of all, the adsorbed carbon can react with water vapor to generate CO and H_2 on the surface of ore. In Step (3), as the Fe shell grows thicker and thicker, the dissolved carbon diffuses down to the Fe/wustite interface to react with wustite. Due to the formation of dense metallic shell, the supply of H_2 gas to the reaction interface becomes difficult, which retarded the production of H_2O. This accelerates the carburization of the metallic shell. Thus, more dissolved carbon can be used to remove the oxygen on the Fe/wustite interface to produce CO gas. Accordingly, the metallic shell formed by CH_4-containing gas is less dense than that by H_2. In Step (4), through the cracks formed in Fe layer by CO generation in Step (3), H_2 easily migrates into the Fe/wustite interface and reduces more FeO, which provides higher fraction reduction of ore towards the end of reduction compared with that by H_2 reduction only. Then high over-pressure of gases is built up inside, which make the Fe layer in loose contact with the wustite.

Carbon content in Fe layer in Fig. 7 was evaluated to be 0.3 to 2.0 mass% by EPMA quantification. The average carbon content is determined by the balance between the carburization by Eq. (22) and decarburization comprising the wustite reduction by Eq. (14) and water-gas reaction by Eq. (23) as follows:

$$H_2O(g) + \underline{C}_{\text{in Fe}} = H_2(g) + CO(g) \quad \text{............} (23)$$
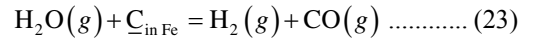
According to Fe–C phase diagram, the carbon content in Fe layer lies in between the solidus and liquidus at $1\,300°C$. Accordingly, the Fe layer should be the mixture of solid and liquid phases. However, as shown in Fig. 11(b), the Fe/wustite interface appears to be relatively less planer, which indicates that the Fe–C layer might be mostly the solid phase as was already estimated by the calculation of the activation energy for the reduction of wustite by CH_4 gas.

4.4. Synergistic Effect of H_2 on the Reduction of the Magnetite Ore by CH_4

As shown in Figs. 5 and 6, the addition of H_2 to CH_4-containing gas made it possible to obtain very high fractional reduction. As expected by Eq. (9), the addition of H_2 thermodynamically decreases the carbon activity of CH_4-containing gas and retards the decomposition of CH_4. However, Ostrovski and Zhang[5] reported that H_2 has an kinetic influence on the increase of initial reduction rate by forming a thin shell of metallic Fe on the oxide surface, which has a catalytic effect on the cracking of CH_4. This indicates that the addition of H_2 to CH_4-containing gas effectively restricts the pre-decomposition of CH_4 and carbon deposition on the particle surface. Consequentially, more CH_4 can participate in the reduction process. In addition, H_2 effectively reduces iron oxide below $1\,100°C$ which is different from CH_4. Accordingly, the addition of H_2 could extend the reduction time as well.

In order to more clearly identify the synergistic effect of H_2 on the reduction of ore by CH_4, additional experiments were carried out by increasing the CH_4 content with H_2 fixed. **Table 4** summarizes the output gas compositions, carbon deposition and fractional reduction for various mixing conditions of input gas. The values in parentheses are equivalent moles which were calculated from volume increase

(1)
Fast reduction from Fe₃O₄ to FeO

(2)
Various chemical reactions on the surface of FeO

(4)
Metallic layer breakdown

(3)
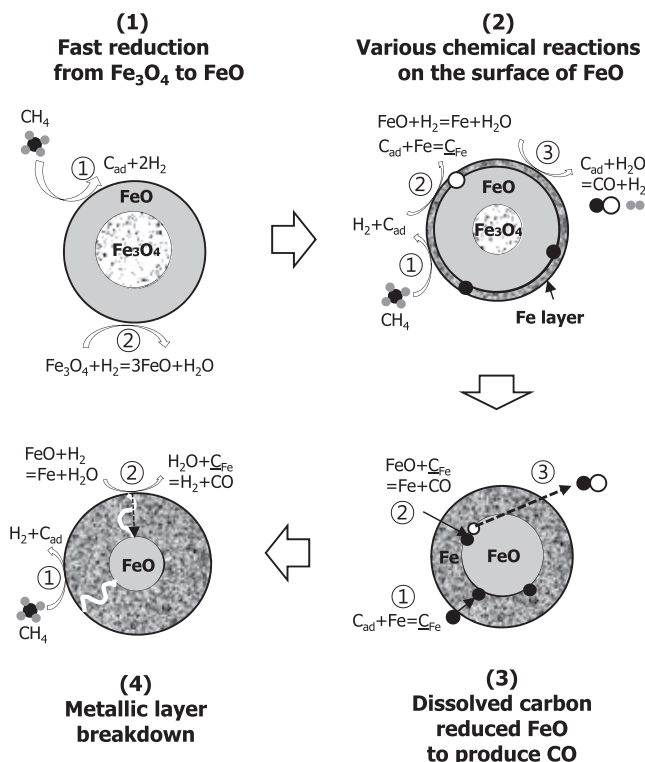**Dissolved carbon reduced FeO to produce CO**

Fig. 12. Illustration of suggested reduction mechanism by CH_4 at $1\,300°C$.

Table 4. Change in output gas compositions, carbon deposition and fractional reduction with varying the composition of input gas mixture at 1 300°C. (mean diameter of ore particles: 50 μm, resident time: 0.7 s).

Input gas vol%=mol% balanced with N_2		Output gas vol% (mol%)			Total volume increase (%)	Results	
CH_4	H_2	CH_4	H_2	CO		Carbon deposition	Fractional Reduction (–)
0	50	0	47.6 (49.5)	3.9 (4.1)	104	–4.1	0.75
3	50	0	51.7 (55.8)	4.3 (4.6)	108	–1.6	0.94
5	50	0.1 (0.1)	53.6 (59.0)	4.8 (5.3)	110	–0.4	0.96
8	50	0.8 (0.9)	56.7 (64.1)	4.8 (5.4)	113	1.7	0.97
11	50	1.7 (1.9)	59.8 (68.2)	4.7 (5.3)	114	3.8	0.94
11	0	0.2 (0.2)	19.0 (21.8)	4.4 (5.1)	115	5.7	0.77

since the values in vol% do not represent the actual change in mass. In addition, the material balance of carbon in between input and output gases did not match since the previously deposited carbon on the wall was consumed by 0–5 vol% CH_4 or additional carbon was deposited by 8–11 vol% CH_4. This indicates that the formation of soot can be solved by adjusting the mixing ratio of CH_4 and H_2. Carbon deposition values in Table 4 indicates that the equilibrium condition was located between 5 and 8 vol% CH_4 for 50 vol%H_2. From very high fractional reductions obtained at the current conditions, the restriction of carbon deposition is very important for not only the prevention of soot but also high fractional reduction. Moreover, the composition of output gas indicates that the output gas can be recycled since the H_2 content was greatly increased by the gasification reaction of carbon with water vapor.

5. Conclusions

The reduction of the Chinese Benxi ore with CH_4-containing gas has been investigated employing suspension reduction technology in the temperature range of 1 100 to 1 300°C. From the findings, the following conclusions were obtained.

(1) The reduction of Benxi magnetite ore by CH_4-containing gas topochemically proceeded to form a metallic Fe shell and its efficiency was greater than that by H_2 or CO at 1 300°C.

(2) It was estimated that the reduction of magnetite ore by CH_4-containing gas could initially be controlled by the chemical reaction to form thin Fe layer. Then with increasing the resident time, the reduction is limited by the wustite reduction with CO which is rapidly provided by the gasification of dissolved carbon at Fe/wustite interface.

(3) The CO gas generated by the wustite reduction with dissolved carbon made great contribution to further reduction of the magnetite ore, which results in forming less dense Fe shell with some cracks in it by gas evolution.

(4) The addition of H_2 to CH_4-containing gas had great influence on the prevention of soot formation and on the achievement of higher reduction degrees of the magnetite ore since the kinetic contribution of H_2 to CH_4 cracking overwhelms the thermodynamic retardation of CH_4 cracking due to the pre-existence of H_2 in gas mixture.

REFERENCES

1) R. J. Fruehan: *New Steel*, **14** (1998), 34.
2) H. Y. Sohn: *Steel Times Int.*, **4** (2007), 68.
3) Y. Nomura, H. Nakagawa, T. Maeda, K. Nishioka and M. Shimizu: *Tetsu-to-Hagané*, **91** (2005), 521.
4) P. J. Read, D. A. Reeve, J. H. Walsh and J. E. Rehder: *Can. Metall. Q.*, **13** (1974), 587.
5) O. Ostrovski and G. Zhang: *AIChE J.*, **52** (2006), 300.
6) N. Takeuchi, Y. Nomura, K. Ohno, T. Maeda, K. Nishioka and M. Shimizu: *ISIJ Int.*, **47** (2007), 386.
7) C. R. Wilke: *J. Chem. Phys.*, **18** (1950), 517.
8) L. A. Haas, J. C. Nigro and R. K. Zahl: Bureau of Mines Report RI-8997, U. S. Department of Interior, Pittsburgh, PA, (1985), 1.
9) A. Steinfeld, A. Frei and P. Kuhn: *Metall. Mater. Trans. B*, **26B** (1995), 509.
10) N. Anacleto and O. Ostrovski: *Metall. Mater. Trans. B*, **35B** (2004), 609.
11) M. E. Choi: Ph D Thesis to the faculty of The University of Utah, (2010), 66, 79.
12) S. Y. Lin, Y. Suzuki, H. Hatano and M. Harada: *Energ. Fuel.*, **15** (2001), 339.
13) H. J. Grabke: *Metall. Trans.*, **1** (1970), 2972.
14) R. J. Fruehan: The Making, Shaping and Treating of Steel, Steelmaking and Refining Volume, 11th ed., AISE Steel Foundation, Pittsburgh, PA, (1998), 20.
15) K. Sugawara, K. Morimoto and T. Sugawara: *AIChE J.*, **45** (1999), 574.
16) H. Szekely, J. W. Ewans and H. Y. Shon: Gas Solid Reactions, Academic Press, New York, (1976), 65, 77.
17) R. J. Fruehan: *Metall. Trans. B*, **8B** (1977), 279.
18) E. T. Turkdogan: *Metall. Trans. B*, **9B** (1978), 163.
19) A. K. Viswas: Principles of Blast Furnace Ironmaking, SBA Pub., Calcutta, India, (1981), 27, 32.
20) D. Ghosh, A. K. Roy and A. Ghosh: *Trans. Iron Steel Inst. Jpn.*, **26** (1986), 186.
21) K. L. Trushenski and W. O. Philbrook: *Metall. Trans.*, **5** (1974), 1149.
22) T. Murayama, Y. Ono and Y. Kawai: *Trans. Iron Steel Inst. Jpn.*, **18** (1978), 579.
23) E. T. Turkdogan and J. V. Vinters: *Metall. Trans.*, **3** (1972), 1561.
24) P. C. Hayes: *Metall. Mater. Trans. B*, **41B** (2010), 19.